

SHEAR RESISTANCE OF ULTRA-HIGH-PERFORMANCE CONCRETE REINFORCED WITH HYBRID STEEL FIBER SUBJECTED TO IMPACT LOADING

Pham Thai Hoan^a, Ngo Tri Thuong^{b,*}

^a*Faculty of Building and Industrial Construction, National University of Civil Engineering, 55 Giai Phong road, Hai Ba Trung district, Hanoi, Vietnam*

^b*Faculty of Civil Engineering, Thuy Loi University, 175 Tay Son street, Dong Da district, Hanoi, Vietnam*

Article history:

Received 23 August 2018, Revised 29 September 2018, Accepted 18 December 2018

Abstract

This study investigated the synergy in shear response of ultra-high-performance fiber-reinforced concrete (UH-PFRCs) containing different contents of long and short smooth steel fiber reinforcements at high strain rates. Shear resistance of two ultra-high-performance mono-fiber-reinforced concrete (UHP-MFRCs): L15S00 (containing 1.5 vol.-% long and 0.0 vol.-% short fiber) or L00S15, and one ultra-high-performance hybrid-fiber-reinforced concrete (UHP-HFRCs): L10S05 (containing 1.0 vol.-% long and 0.5 vol.-% short fiber) at high strain rates of up to 272 s^{-1} was investigated using a new shear test setup by an improved strain energy frame impact machine (I-SEFIM). The L10S05 generated high synergy in shear strength, shear peak toughness at static rate and high synergy in shear strain, shear peak toughness at high strain rates. Moreover, all the investigated UHPFRCs were sensitive to the applied strain rates, especially in term of shear strength.

Keywords: UHPFRCs; shear resistance; synergy effect; strain-rate dependent; impact.

[https://doi.org/10.31814/stce.nuce2019-13\(1\)-02](https://doi.org/10.31814/stce.nuce2019-13(1)-02) © 2019 National University of Civil Engineering

1. Introduction

Ultra-high-performance fiber-reinforced concrete (UHPFRC) is a potential material for wide use in protective structures for aeronautics, nuclear industry, and military buildings as a safeguard against impact or blast loading, owing to its superior mechanical characteristics such as very high compressive strength [1], high tensile strength, ductility [2], and energy absorption capacity [3]. Nevertheless, the application of UHPFRCs to civil infrastructures is still very limited because of their relatively high fiber contents and cost [4, 5]. It is necessary to reduce the fiber contents as well as the cost of the UHPFRCs, without sacrificing their high mechanical resistance and work ability.

Several methods have been carried out to reduce the fiber content and cost of UHPFRCs, which may be listed as follows: (1) increasing mechanical interfacial bond strength between fiber and matrix by utilizing deformed steel fiber geometries [6]; (2) generating synergistic responses by blending of long and short fibers reinforcements [5]; and (3) enhancing the physical and chemical bond strength between the fiber and matrix by maximizing packing density of the matrix [7]. Among the various methods, blending long and short fibers has been proven as one of the most effective methods, owing to a combination of various features from those different fiber reinforcements [8, 9]. For example,

*Corresponding author. *E-mail address:* trithuong@tlu.edu.vn (Thuong, N. T.)

the shorter reinforcements can effectively restrict the development of micro-cracks while the longer reinforcements can bridge macro-cracks [10].

Even though the mechanical properties of ultra-high-performance hybrid-fiber-reinforced concrete (UHP-HFRC) have been intensively investigated by many researchers, researchers have mostly focused on the compressive [9–12], tensile [5, 13, 14], and flexural [15, 16] properties of UHP-HFRCs rather than their shear resistance [16]. Moreover, most previous studies have focused on the quasi-static properties [9, 12, 13] rather than the impact behavior [5, 10, 11, 14, 16].

Wu et al. [10] used the split Hopkinson press bar (SHPB) testing to investigate the static and dynamic compressive strength of UHP-HFRCs and found that the UHP-HFRC containing 1.5% fiber volume content (1.5 vol.-%) long and 0.5 vol.-% short steel fiber reinforcements exhibited higher compressive strength than those containing only 2.0 vol.-% of long or short fibers, at both static and high strain rates. Millard et al. [16] used drop-hammer techniques to investigate the dynamic increase factor (DIF) under both flexural and shear loading of UHP-HFRCs. The results showed that the beam containing 6 vol.-% long and short steel fibers produced the lowest dynamic increase factor (DIF) under flexural loading, whereas there is no significant strain rate enhancement in the case of shear loading. Tran et al. [5] investigated the synergistic response of blending fibers in UHPC under high rate tensile load using a strain energy frame impact machine (SEFIM). They have reported that the blending of long and shorter steel fibers in UHPC generated notable synergistic effects on the tensile response of UHP-HFRCs, especially at high strain rates. Until now, there is still little available information about the effect of fiber hybridization on the shear resistance of UHPFRCs, especially at high strain rates.

This study aims to understand the influence of synergistic response and strain rates on the shear resistance of UHPFRCs using the new shear test method, recently developed by Ngo et al. [17], that is capable of measuring the shear-related hardening response of UHPFRCs, accompanied by multiple microcracks. The first one of the two main objectives in this study is to examine the synergistic responses on the shear resistance of UHP-HFRCs and the second objective is to investigate the strain rate effect on the shear resistance of UHPFRCs.

2. Experimental program

Three series of prism shear specimen named as L15S00 (containing 1.5 vol.-% long and 0.0 vol.-% short fiber), L00S15 (containing 0.0 vol.-% long and 1.5 vol.-% short fiber), and L10S05 (containing 1.0 vol.-% long and 0.5 vol.-% short fiber) with the same UHPC matrix were prepared and tested. Each specimen series consists of 6 specimens, leading to the total of 18 prism specimens with the same size of $50 \times 50 \times 210 \text{ mm}^3$.

2.1. Material and specimen preparation

The composition by weight ratio of Ultra-high-performance (UHPC) matrix is listed in Table 1 while the properties of long and short smooth steel fibers are listed in Table 2. The silica sand and the silica fume are first to dry mixed for 5 mins. The cement and the silica powder are then added and mixed in approximately more 5 mins. The water and superplasticizer are slowly added with 2 mins interval and mixed continuously until the mixture showed adequate workability. Finally, the fibers are carefully poured by hand into the mixture while the mixer machine kept rotating for 2 mins. Detail of the mixing procedure can be found in the previous work [17].

The UHPFRC mixture is cast into plastic molds by a scoop without vibration before storing in the laboratory temperature for 48 h. The specimens are demolded and cured in the hot water tank at 90

Table 1. The composition of UHPC matrix by weight ratio

Cement (Type I)	Silica fume	Silica sand	Silica powder	Super-plasticizer	Water
1	0.25	1.10	0.30	0.067	0.2

Table 2. Properties of smooth steel fibers

Fiber type	Diameter, d_f (mm)	Length l_f (mm)	Density, ρ (g/cc)	Tensile strength, μ_u (MPa)	Elastic modulus, E (GPa)
Short smooth steel fiber	0.2	13	7.90	2788	200
Long smooth steel fiber	0.2	19	7.90	2580	200

$\pm 2^\circ\text{C}$ in 72 h. All specimens were tested at the ages of 28 days. The compressive strength of UHPC matrix was 189 MPa according to [18].

2.2. Test setup and procedure

In order to investigate the synergistic responses and the strain rate effect on the shear resistance of UHPFRCs, shear tests were conducted at both static and high strain rates. Static shear tests were carried out on three specimens of each specimen series, which were denoted by the “-S” notation following the name of each series, whereas the dynamic shear tests were carried out on three remaining specimens of each series, which were denoted by the “-H” notation following the name of each series.

Fig. 1 shows the static shear test system. The shear test setup, recently proposed by Ngo et al. [17], was employed in the universal test machine (UTM) to implement the static shear test. Details of the shear test setup could be found in [17]. The speed of machine displacement was maintained as 1 mm/min during static shear testing. The applied load was measured by a load cell installed inside the UTM, while the displacement was recorded by two linear variable displacement transducers (LDVTs) attached to the bottom surface of the specimen by an aluminum frame, as can be seen in Fig. 1.

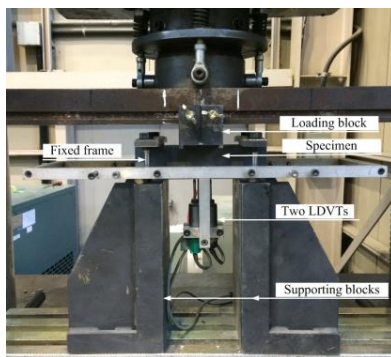


Figure 1. Static shear test setup

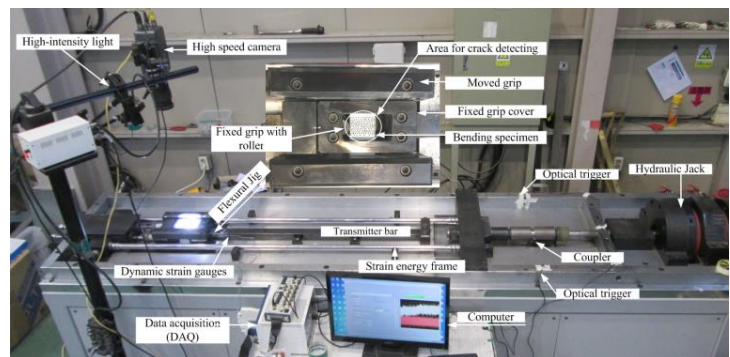


Figure 2. Impact shear test setup

Fig. 2 shows the shear test machine at high strain rates. A shear test setup with the same specimen size and boundary conditions as the static shear test was employed in an improved strain energy frame impact machine (I-SEFIM) to investigate the shear resistance of UHPFRCs at high strain rates. The detail of shear impact system could be found elsewhere [19]. The shear stress was obtained from two

dynamic strain gauges attached on the surfaces of the transmitter bar, while the shear strain of the specimen was measured from the relative displacement of marked points on a fixed grip and a moved grip by a high-speed camera system, as shown in Fig. 2. The speed of applied load was controlled by the capacity of coupler and types of energy frame: the coupler with 800 kN capacity and high strength steel energy frame were used in this study.

3. Results

The shear stress-versus-strain of UHPFRCs at the different strain rates is shown in Fig. 3, while their shear parameters are listed in Table 3. The equations to calculate the shear strength, shear strain capacity, strain rates, and shear peak toughness can be referred in [19]. Generally, the shear resistance of UHPFRCs increased as the applied strain rates increased, although the shear parameters were strongly dependent on the combination of fiber reinforcements. The L10S05 exhibited the highest shear strength (τ_{\max}) and shear peak toughness (T_{sp}) at static rate. The average τ_{\max} of L00S15, L10S05, and L15S00 are 18.2, 24.4, and 20.8 MPa, while T_{sp} of those are 0.51, 0.89, and 0.76 MPa, respectively. Their γ_{\max} are 0.045, 0.050, and 0.054 as listed in Table 3. However, the shear strength (31.9 MPa) of L15S00 is significantly higher than those of the L10S05 (30.1 MPa) and the L00S15 (26.80 MPa) at high strain rates. In addition, the L10S05 produced the highest value in terms of the shear strain and the shear peak toughness. Their values of γ_{\max} and T_{sp} are 0.088 and 1.40 MPa for the L00S15, 0.107 and 1.91 MPa for the L10S05, and 0.06 and 1.12 MPa for the L15S00.

Failure of the specimens is shown in Fig. 4. All specimens failed with two major shear cracks, accompanied by the formation of multiple-micro cracks. In addition, the number of cracks at high strain rates (Fig. 4(a)) was significantly higher than at static rates (Fig. 4(b)).

4. Discussions

4.1. Synergistic effect of blending long and short fiber on shear resistance of UHP-HFRCs

The synergy evaluation of UHP-HFRCs using Eq. (1) is shown in Fig. 5. The Eq. (1) defines synergy as the amount by which the performance of a hybrid system exceeds that of each mono-component system as the same fiber volume content [5]:

$$S = \frac{R_{\text{hybrid},a+b}^{(V_f)} - \max(R_{\text{mono},a}^{(V_f)}, R_{\text{mono},b}^{(V_f)})}{\max(R_{\text{mono},a}^{(V_f)}, R_{\text{mono},b}^{(V_f)})} \quad (1)$$

where $R_{\text{hybrid},a+b}^{(V_f)}$ is the shear resistance of UHP-HFRC reinforced with fiber a and b , $R_{\text{mono},a}^{(V_f)}$, $R_{\text{mono},b}^{(V_f)}$ are the shear resistance of ultra-high-performance mono-fiber-reinforced concrete (UHP-MFRC) containing fiber a and b , respectively. Notably, the UHP-HFRCs and UHP-MFRCs have the same total fiber volume content, V_f . A positive value of “S” indicates that the hybrid system performs better than the mono system or the sum of individual fibers.

As can be seen in Fig. 5, the UHP-HFRC containing 1.0 vol.-% long fiber and 0.5 vol.-% short fiber (L10S05) exhibited the positive synergy values for the shear strength (τ_{\max}), shear peak toughness (T_{sp}), but the negative synergy value for the shear strain capacity (γ_{\max}), at static rate. Whereas they produced the best synergy in the T_{sp} , at high strain rates. Specifically, the synergy values for τ_{\max} , γ_{\max} and T_{sp} of L05S10 were 0.175, -0.075 , and 0.160 at the static rate, and -0.056 , 0.218, and 0.367 at the high strain rates, respectively. The reason for the synergy effect of the UHPFRCs at static

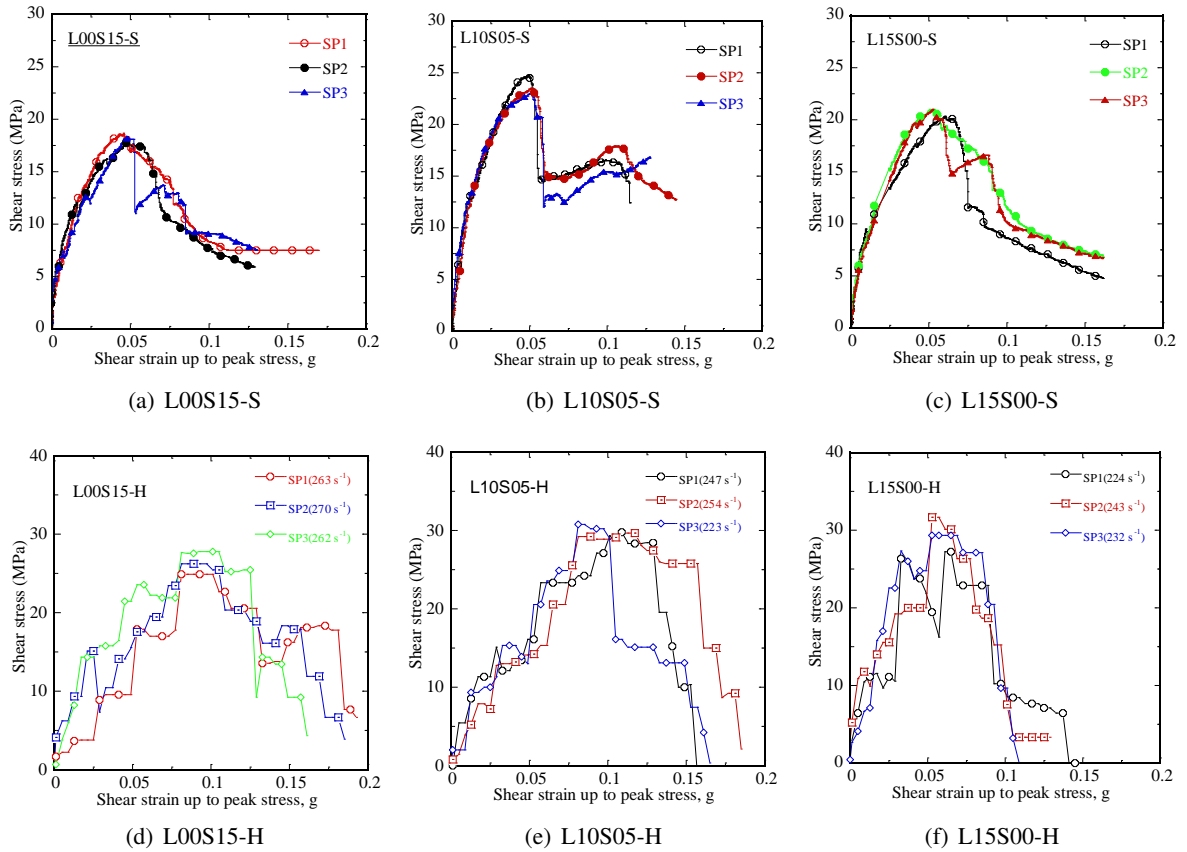


Figure 3. Shear stress-versus-strain of UHPFRCs at different strain rates



(a) Static rates

(b) High strain rates

Figure 4. Typical failure of shear UHPFRCs specimens

rates was different from the high strain rates is not really clear but likely related to the difference in crack propagate mechanism in the UHPFRC specimens under different applied strain rates. Unlike at the static rates, the micro and macro cracks almost happen at the same time owing to the extreme load speeds. The difference in the strain-rate sensitivity characteristics of the long and short fiber might be another reason for the different synergy effect between static and high applied strain rates. The synergy response of the L10S05 under shear loading, in this study, was the same as those under direct tensile loads at high strain rates. Tran et al. [5] investigated the synergy response of the L10S05, under static and high strain rate direct tensile loads, reported that the L10S05 exhibited the negative effects

Table 3. Test results

Test series	Specimen	Strain rate		Shear strength, τ_{\max}		Shear strain at peak stress, γ_{\max}		Shear peak toughness, T_{sp}	
		Type	s^{-1}	MPa	DIF	DIF	MPa	DIF	
L00S15-S	SP1	Static	0.000667	18.63	-	0.045	-	0.59	-
	SP2			17.92	-	0.048	-	0.51	-
	SP3			18.02	-	0.042	-	0.42	-
	Average SD	0.000667	18.2 0.4	1.0	0.045 0.003	1.0	0.51 0.08	1.0	
L10S05-S	SP1	Static	0.000667	24.80	-	0.049	-	0.93	-
	SP2			23.57	-	0.050	-	0.93	-
	SP3			24.80	-	0.051	-	0.79	-
	Average SD	0.000667	24.4 0.7	1.0	0.050 0.001	1.0	0.89 0.08	1.0	
L15S00-S	SP1	Static	0.000667	20.33	-	0.060	-	0.84	-
	SP2			20.98	-	0.051	-	0.72	-
	SP3			20.99	-	0.053	-	0.73	-
	Average SD	0.000667	20.8 0.4	1.0	0.054 0.005	1.0	0.76 0.06	1.0	
L00S15-H	SP1	High rates	235	26.93	1.48	0.080	1.77	1.44	2.86
	SP2		260	26.11	1.44	0.104	2.31	1.59	3.15
	SP3		270	27.22	1.50	0.079	1.75	1.15	2.28
	Average SD	257	26.8 0.6	1.47	0.088 0.014	1.94	1.40 0.22	2.76	
L10S05-H	SP1	High rates	272	29.81	1.24	0.105	1.95	1.65	2.04
	SP2		254	29.71	1.22	0.078	1.56	1.27	1.66
	SP3		223	30.80	1.26	0.136	2.71	2.81	3.68
	Average SD	230	30.1 0.6	1.2	0.107 0.029	2.1	1.91 0.80	2.5	
L15S00-H	SP1	High rates	224	30.00	1.44	0.059	1.09	0.93	1.22
	SP2		243	33.10	1.59	0.052	0.96	0.85	1.11
	SP3		232	32.59	1.57	0.069	1.27	1.59	2.08
	Average SD	232	31.9 1.7	1.5	0.060 0.008	1.1	1.12 0.41	1.5	

in term of post-cracking strength (σ_{pc}), but highly effective in terms of tensile strain capacity (ε_c) and peak toughness (T_p).

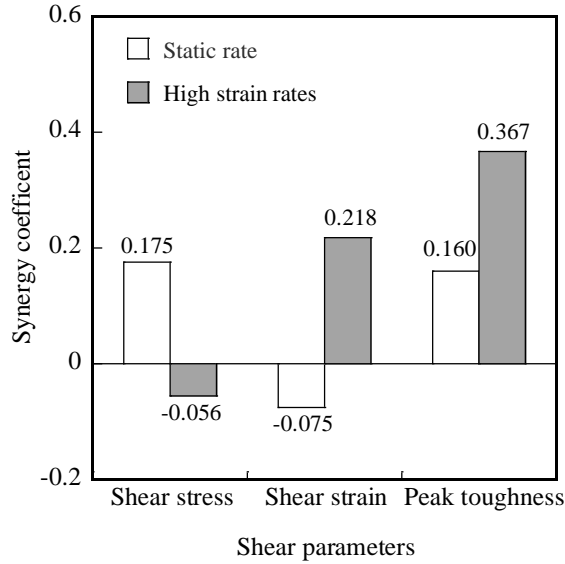


Figure 5. Synergistic response of UHP-HFRCs

4.2. High strain rate effect on shear resistance of UHPFRCs

The DIFs, ratio between the dynamic and static responses, of the shear parameters (τ_{max} , γ_{max} , T_{sp}) of UHPFRCs at high strain rates (up to 272 s^{-1}) are plotted in Fig. 6, including DIFs for shear strength (Fig. 6(a)), shear strain capacity (Fig. 6(b)), and shear peak toughness (Fig. 6(c)). Generally, the UHPFRCs were found to be sensitive to the applied strain rates. As the strain increased from the static rate (0.000667 s^{-1}) to the high strain rates (up to 272 s^{-1}), the DIFs of τ_{max} of the L00S15, L10S05, and L15S00 were 1.47, 1.20, and 1.50, while the DIFs of γ_{max} were 1.94, 2.10, and 1.10, respectively. Those DIFs of T_{sp} , which is shown in Fig. 6(c) were 2.76, 2.50, and 1.50.

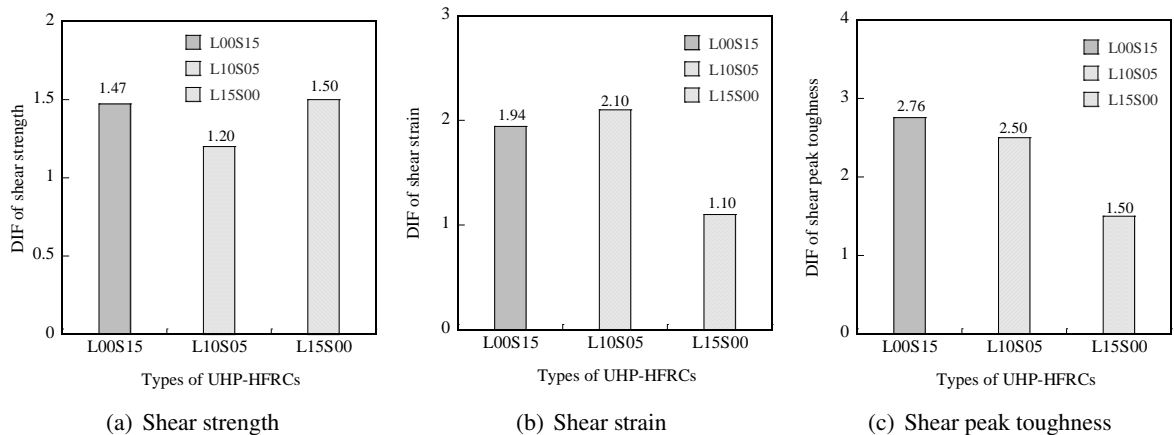


Figure 6. Strain rate effect on shear resistance of UHPFRCs

The average DIF (1.50) of the L15S00 for τ_{max} at high strain rate up to 272 s^{-1} was found to be significantly lower than those of tensile strength. The DIF of the tensile strength (σ_{pc}) of UHPFRC containing 1.5 vol.-% short steel fibers was reported as about 3.0 at the high strain rate of 21.4 s^{-1}

[5]. The lower rate sensitivity of τ_{max} , in comparison with the σ_{pc} of UHPFRCs, was also reported and explained by [19] owing to the lower inertial effect, in the shear specimen, of mortar matrix surrounding fibers.

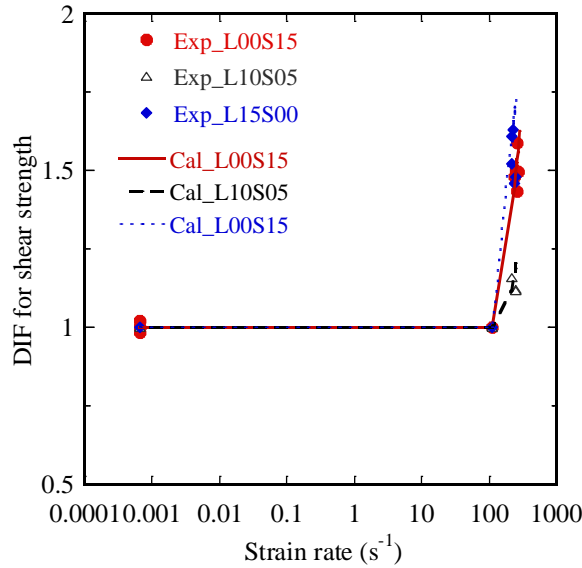


Figure 7. Strain rate effect on shear resistance of UHPFRCs

Fig. 7 plots the experimental shear strength (τ_{exp}) and calculated shear strength (τ_{cal}) of UHPFRCs at high strain rates. In which, the τ_{cal} was calculated by a proposed equation of [19], as Eq. (2):

$$DIF_{\tau_{max}} = \begin{cases} 1 & \dot{\gamma}_s < \dot{\gamma} \leq 110/s \\ 0.07023 \times (\dot{\gamma})^{0.582} & \dot{\gamma} > 110/s \end{cases} \quad (2)$$

where $DIF_{\tau_{max}}$ is the DIFs for the shear strength, $\dot{\gamma}_s$ is static strain rate (0.000667 s^{-1} in this study), and $\dot{\gamma}$ is the applied shear strain rates. Notably, the coefficient 0.07023 in Eq. (2) was kept for the L15S00 and justified to 0.06 for the L00S15 and 0.048 for the L10S05, respectively, while the exponent (0.582) was maintained. As demonstrated in Fig. 7, the shear strength of all investigated UHPFRCs could be predicted by using the empirical proposed by [17].

5. Conclusions

The effects of blending fibers on the shear resistance of UHPFRCs at both static and higher strain rates were investigated using a new shear test method. Specimens with the same size and boundary conditions were used at both static and high strain rates to minimize the potential effects of inertia and boundary conditions on the test results. The following observations and conclusions can be drawn from this study:

- All the investigated UHPFRCs were sensitive to the applied strain rate, especially the L15S00.
- The L10S05 generated high synergy in shear strength, shear peak toughness at static rate, but high synergy in shear strain and shear peak toughness at high strain rates.

Acknowledgement

This research is funded by Vietnam National Foundation for Science and Technology Development (NAFOSTED) under grant number 107.01-2018.22.

References

- [1] Wille, K., Naaman, A. E., Parra-Montesinos, G. J. (2011). Ultra-High Performance Concrete with Compressive Strength Exceeding 150 MPa (22 ksi): A Simpler Way. *ACI Materials Journal*, 108(1).
- [2] Wille, K., Kim, D. J., Naaman, A. E. (2011). Strain-hardening UHP-FRC with low fiber contents. *Materials and Structures*, 44(3):583–598.
- [3] Kang, S.-T., Lee, Y., Park, Y.-D., Kim, J.-K. (2010). Tensile fracture properties of an Ultra High Performance Fiber Reinforced Concrete (UHPFRC) with steel fiber. *Composite Structures*, 92(1):61–71.
- [4] Yoo, D.-Y., Kim, S., Park, G.-J., Park, J.-J., Kim, S.-W. (2017). Effects of fiber shape, aspect ratio, and volume fraction on flexural behavior of ultra-high-performance fiber-reinforced cement composites. *Composite Structures*, 174:375–388.
- [5] Tran, N. T., Kim, D. J. (2017). Synergistic response of blending fibers in ultra-high-performance concrete under high rate tensile loads. *Cement and Concrete Composites*, 78:132–145.
- [6] Wille, K., Naaman, A. E. (2010). Fracture energy of UHPFRC under direct tensile loading. In *FraMCoS-7 International Conference*, 65–72.
- [7] Kim, D. J., Wille, K., Naaman, A. E., El-Tawil, S. (2012). Strength dependent tensile behavior of strain hardening fiber reinforced concrete. *RILEM Bookseries*, 2:3–10.
- [8] Hannawi, K., Bian, H., Prince-Agbodjan, W., Raghavan, B. (2016). Effect of different types of fibers on the microstructure and the mechanical behavior of ultra-high performance fiber-reinforced concretes. *Composites Part B: Engineering*, 86:214–220.
- [9] Wu, Z., Shi, C., He, W., Wu, L. (2016). Effects of steel fiber content and shape on mechanical properties of ultra high performance concrete. *Construction and Building Materials*, 103:8–14.
- [10] Wu, Z., Shi, C., He, W., Wang, D. (2017). Static and dynamic compressive properties of ultra-high performance concrete (UHPC) with hybrid steel fiber reinforcements. *Cement and Concrete Composites*, 79:148–157.
- [11] Yu, R., Spiesz, P., Brouwers, H. J. H. (2014). Static properties and impact resistance of a green Ultra-High Performance Hybrid Fibre Reinforced Concrete (UHPHFRC): experiments and modeling. *Construction and Building Materials*, 68:158–171.
- [12] Wu, Z., Shi, C., He, W., Wang, D. (2016). Uniaxial compression behavior of ultra-high performance concrete with hybrid steel fiber. *Journal of Materials in Civil Engineering*, 28(12):06016017.
- [13] Park, S. H., Kim, D. J., Ryu, G. S., Koh, K. T. (2012). Tensile behavior of ultra high performance hybrid fiber reinforced concrete. *Cement and Concrete Composites*, 34(2):172–184.
- [14] Park, J. K., Kim, S.-W., Kim, D. J. (2017). Matrix-strength-dependent strain-rate sensitivity of strain-hardening fiber-reinforced cementitious composites under tensile impact. *Composite Structures*, 162: 313–324.
- [15] Kim, D. J., Park, S. H., Ryu, G. S., Koh, K. T. (2011). Comparative flexural behavior of hybrid ultra high performance fiber reinforced concrete with different macro fibers. *Construction and Building Materials*, 25(11):4144–4155.
- [16] Millard, S. G., Molyneaux, T. C. K., Barnett, S. J., Gao, X. (2010). Dynamic enhancement of blast-resistant ultra high performance fibre-reinforced concrete under flexural and shear loading. *International Journal of Impact Engineering*, 37(4):405–413.
- [17] Ngo, T. T., Park, J. K., Pyo, S., Kim, D. J. (2017). Shear resistance of ultra-high-performance fiber-reinforced concrete. *Construction and Building Materials*, 151:246–257.
- [18] Ngo, T. T., Kim, D. J., Moon, J. H., Kim, S. W. (2018). Strain rate-dependent shear failure surfaces of ultra-high-performance fiber-reinforced concretes. *Construction and Building Materials*, 171:901–912.
- [19] Ngo, T. T., Kim, D. J. (2018). Shear stress versus strain responses of ultra-high-performance fiber-reinforced concretes at high strain rates. *International Journal of Impact Engineering*, 111:187–198.